International Journal of Applied Engineering Research ISSN 0973-4562 Volume 13, Number 5 (2018) pp. 2882-2891

Modeling of the Effect of Process Parameters on Tensile Strength of Friction Stir Welded Rare Earth ZE-41 Magnesium Alloy Joints

Bhupinder Singh [1], Kulwant Singh [2] and V. Sahni [3]

[1] *Assistant Professor, Department of Mechanical Engineering, Guru Nanak Dev Engineering College, Ludhiana-141006, Punjab India.*

[2, 3] *Professor, Department of Mechanical Engineering, Sant Longowal Institute of Engineering & Technology, Longowal, Sangrur-148106, Punjab, India.*

Abstract

The recently developed rare earth containing magnesium alloy ZE-41 is gaining wide spread applications in automobile, aerospace and defense sectors due to its high-quality formability and more strength to weight ratio. Magnesium is normally known as complicated to join material by fusion welding processes owing to defects encountered in fusion welded joints such as inclusions, cracks, porosity, and distortions. Innovative technique, friction stir welding is a capable solid state joining process for successful joining of Mg alloys. The process parameters affecting joint properties of weldments are downward axial force, tool pin geometry, tool rpm and weld speed. In present investigation magnesium alloy friction stir weldments were fabricated with five different tool geometries. Total 31 experiments with 4 factors, 5 levels were conducted as per central composite design matrix. Mathematical model was developed from the data generated by using response surface method. Adequacy for the developed model was checked by means of ANOVA method. Major and interactive influences of welding parameters on tensile behavior are described with the help of graphs for better understanding. It was revealed that the straight cylindrical pin have the highest tensile properties. Mathematical model is useful for the prediction of tensile strength for controlling the weld quality by selecting appropriate process parameters for rare earth containing ZE41 magnesium alloy.

Keywords: ZE-41Mg alloy, rare earth, friction stir welding, mathematical modeling, ultimate tensile properties.

INTRODUCTION

Magnesium alloys are becoming more and more popular in aircraft and automotive industries due to their light weight as compared to Al alloys and high strength to weight ratio [1]. Mg alloys are center of attention for the researchers who are actively involved in welding of such alloys because poor response of magnesium alloys to usual fusion welding methods. Main difficulties occurring during fusion welding of Mg alloys are cracks, porosity formation, oxide inclusions and distortions but these defects can be eliminated by using solid state joining method known as FSW, which is relatively new entrant in welding processes[2].ZE-41Mg alloy containing rare earth elements ytterbium and zirconium which results in various advantages such as purifying the alloy, enhancing cast-ability, modifying the grain size and microstructure, enhances the mechanical and anti-oxidation behavior. For achieving high temperature strength, creep resistance and high formability rare earth elements are added into Mg alloys [3-5]. Due to high demand for energy saving and environmental protection throughout the world magnesium is gaining praise as a green engineering material [6].The magnesium alloys react readily with oxygen in melting temperature ranges therefore it is preferred to perform welding of Mg alloys at lower temperature in solid state. Hence, FSW is most suitable welding process for defect free joining of magnesium alloys [7]. FSW prevents difficulties related to solidification while joining Mg alloys because the welding is carried out in solid state. High temperature stresses and distortions are also lower in comparison to the usual joining processes. P.Carlone [8] carried out analysis of GTAW and FSW for ZE-41A Mg alloy and reported that by adopting spindle speed of 1000 rpm and 120 mm/min of weld speed, sound joints can be achieved. The correlation exists between the precipitate grain size and microhardness of weldment in FS welded AE42 Mg alloy [9]. Chai et al. [10] investigated submerged friction stir processing and they reported refinement in micro-structure and enhancement in mechanical behavior of AZ91 Mg alloy. Ugender et al. [11] reported that tool rpm and machine tool pin material affected the tensile behavior and microstructure of the obtained FSW joints. Another study by Singh et al. [12] reported enhancement in the impact toughness and tensile behavior of the weldments as compared to parent material AZ31B by using friction stir welding. Seung et al. [13] observed that the leading side was the weakest part in the joint due to change in grain orientation because most of the joint failure occurred at the boundary between TMAZ at leading side and the SZ in all the joints. With increase in rotational speed and by decreasing the travel speed generated higher heat input in stir zone hence enhanced the grain growth [14].To predict the response within given set of operational parameters more precisely and effectively a variety of experimental design techniques are available.

Taguchi technique with an orthogonal array was used to reduce the number of experiments. Drawback of this method is that a few interactions with variables, which can be overcome by response surface methodology [15-16]. Sankar et al. [17] applied 3 factors 5 level central composite design by using RSM to AA6061 alloy and reported that hardness of the joints first increases up to 1120 rpm and then decreases. Singh et al. [18] developed mathematical models for prediction of UTS of Al alloy FS welded joints with central composite rotatable design.

Nowadays extensive research is going for the possibility of joining Al and zinc based magnesium alloys mainly AZ61, AZ31, AZ91 and AZ81 series [19-26]. Although, limited studies have been carried to explore the possibility of joining ZE-41 Mg alloy but influence of process parameters on tensile strength have not been investigated. Moreover mathematical modeling of the process parameters have not been reported so for. So to plug the above gap, present research has been carried out.

MATERIALS AND METHODS

Magnesium alloy ZE-41 plates 150×75 mm and 6 mm thickness were used to make the weld joints as shown in Fig. 1. The chemistry and mechanical behavior of Mg alloy is given in Table 1 and Table 2. The CNC FSW machine manufactured by R.V machine tools, having 15 HP of main spindle, maximum tool speed of 3000 rpm and maximum axial force 25kN was used.

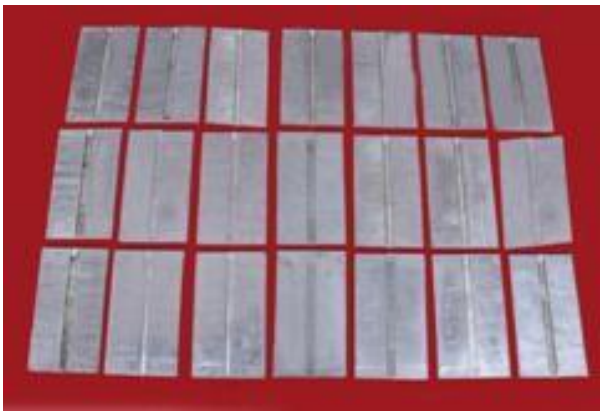

Figure 1: F.S welded joints of ZE-41

Five tools having different pin geometry as shown in Fig. 2 made from high percentage carbon steel were selected to weld the joints. Four independently controllable process parameters having profound effect on UTS of the joints as shown in Table 3, along with notations and their working range, were used. The design matrix have been developed using central composite design. The developed design matrix for 4 factors 5 levels factorial design consisting 31 experiments comprising of 2^4 (=16) factorial design plus 7 center points and 8 star points. All the welding process parameters at the middle level (0) represent center points, whereas a combinations of each welding parameter at its lower value (-2) or higher value (+2) with the other 4 welding parameters at the middle level represent the star points. The developed design matrix is given in Table 4. Therefore the total 31 experimental runs permitted the evaluation of quadratic and two way interactive effects of the welding parameters on the ultimate tensile strength.

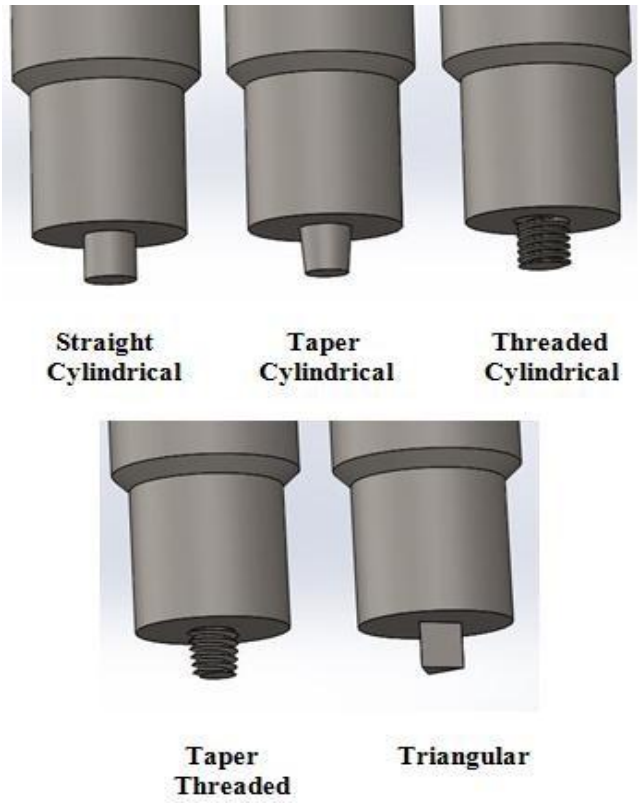

Figure 2: Various tool pin geometries used for making joints

The work pieces were welded in a single pass using threaded cylindrical (THC), triangular (T), taper cylindrical (TC), taper threaded (TT), straight cylindrical (SC) tools with diameter of shoulder 18 mm and length of tool pin 5.7 mm. For better weld quality of the joints and less tool wear rate, HCS tool material was selected for this research work. As estimated from the design matrix, total 31 joints were fabricated. ASTM E8M-04 specifications were used to prepare the tensile test specimens as shown in Fig. 3. Three specimens were taken from the center of each weld length as shown in Fig. 4. The tensile test was performed on a UTM having maximum capacity of 50kN at a loading rate of 1.5 mm/min. The tensile behavior of the joints has been recorded in Table 4. For metallurgical investigations, metallographic specimens were prepared using a standard procedure. The etching reagent was prepared by adding 10g Citric acid in 90 ml water. Microstructural analysis was carried out by SEM (Carl Zeiss Germany Model: Ultra plus 55) to reveal the changes in microstructure of the joints.

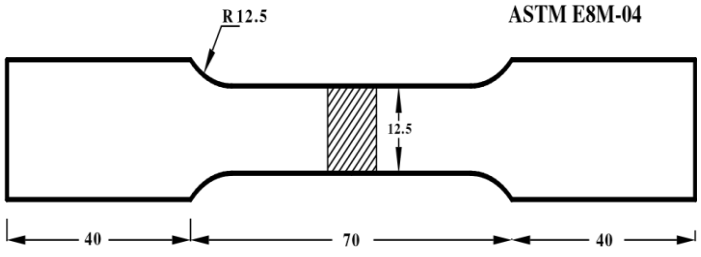

Figure 3: Dimensions of tensile specimen

Table 1: Chemistry of ZE-41 Mg alloy used

Alloy	Element	Zr	Zn	Yb	Mg
ZE-41	Wt. (%)	0.68	4.8	0.51	Balance

Table 2: Mechanical behavior of parent material ZE-41

UTS (MPa)	Change in length (%)	Reduction in area (%)	Hardness VHN
145	3	3	113

Table 3: Process parameters used

Coded levels	Tool Speed (N) rpm	Welding Speed (S) mm/min	Axial Force (F) kN	Pin Profile (P)
-2	1200	10	2	THC
-1	1300	20	3	T
0	1400	30	4	TC
+1	1500	40	5	TT
+2	1600	50	6	TC

THC: Threaded cylindrical, T:Triangular,

T.C: Taper cylindrical, T.T: Taper threaded,

S.C: Straight cylindrical.

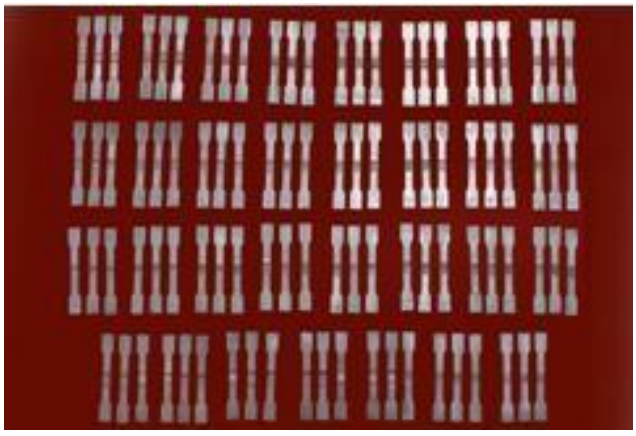

Figure 4: Specimens for tensile testing

Developing Mathematical Model

From the data generated during this experimentation, mathematical model was developed which is useful for accurately predicting UTS. Response surface method was used to develop mathematical equations related to response characteristics and welding variables. Thirty one experiments as shown in Table 4 were performed.

Table 4: Developed design matrix and UTS values

Trial runs	FSW variables				UTS (MPa)
	N	S	F	P	
1	-1	-1	-1	-1	144
2	+1	-1	-1	-1	154
3	-1	+1	-1	-1	150
4	+1	+1	-1	-1	153
5	-1	-1	+1	-1	150
6	+1	-1	+1	-1	164
7	-1	+1	+1	-1	153
8	+1	+1	+1	-1	157
9	-1	-1	-1	+1	160
10	+1	-1	-1	+1	162
11	-1	+1	-1	+1	172
12	+1	+1	-1	+1	165
13	-1	-1	+1	+1	157
14	+1	-1	+1	+1	159
15	-1	+1	+1	+1	158
16	+1	+1	+1	+1	155
17	-2	0	0	0	154
18	+2	0	0	0	163
19	0	-2	0	0	151
20	0	+2	0	0	154
21	0	0	-2	0	155
22	0	0	+2	0	157
23	0	0	0	-2	159
24	0	0	0	+2	167
25	0	0	0	0	163
26	0	0	0	0	165
27	0	0	0	0	163
28	0	0	0	0	162
29	0	0	0	0	161
30	0	0	0	0	163
31	0	0	0	0	162

The selected process parameters were changed up to five levels. The response function, ultimate tensile strength (UTS) of the joints is function of rotational speed (N), welding speed (S), axial force (F) and tool pin profile (P). The response can be expressed as:

$$UTS = f(N, S, F, P) \quad (1)$$

To represent the response surface regression equation of second order polynomial is given by:

$$UTS = b_0+\Sigma b_i x_i+\Sigma b_{ii} x_i^2+\Sigma b_{ij} x_i x_j \quad (2)$$

The preferred polynomial for 4 factors can be written as:

$$UTS = b_0+b_1N+b_2S+b_3F+b_4P+b_{11}N_2+b_{22}S_2+b_{33}F_2+b_{44}P_2 +b_{12}NS+b_{13}NF+b_{14}NP+b_{23}SF+b_{24}SP +b_{34}FP \quad (3)$$

The average of responses is b_0 and b_1, b_2, b_3 and b_4 are the coefficients of linear terms, and b_{11}, b_{22}, b_{33}, b_{44} are the coefficients of quadratic terms, and b_{12}, b_{13}, b_{14}, b_{23}, b_{24} and b_{34} are the coefficients of interactive terms. The coefficients of polynomial equation (4) were derived with the help of design expert software. After dropping insignificant coefficients and putting significant coefficients in equation 4, the developed model is:

$$UTS= 162.71+1.79N+0.79S+3.29P-1.94NS-2.31NP-1.69SF -3.31FP-1.13N^2-2.63S^2-1.75F^2 \quad (4)$$

Adequacy testing of developed model

The analysis of variance technique (ANOVA) was used for checking the adequacy of the developed model as shown in Table 5.

Table 5: ANOVA for developed model

Source	Sum of Squares	d.f	Mean square	F Value	p-value Prob. >F
Model	**1013.17**	**14**	**72.37**	**24.89**	**.0001**
A-Tool Rotational Speed	77.04	1	77.04	26.50	.0001
B-Welding Speed	15.04	1	15.04	5.17	.0370
C- Axial Force	0.37	1	0.37	0.13	.7242
D-Pin Profile	260.04	1	260.04	89.45	.0001
AB	60.06	1	60.06	20.66	.0003
AC	5.06	1	5.06	1.74	.2055
AD	85.56	1	85.56	29.43	.0001
BC	45.56	1	45.56	15.67	.0011
BD	7.56	1	7.56	2.60	.1263
CD	175.56	1	175.56	60.39	.0001
A_2	36.29	1	36.29	12.48	.0028
B_2	197.27	1	197.27	67.86	.0001
C^2	87.72	1	87.72	30.18	.0001
D^2	6.33	1	6.33	2.17	.9963
Residual	**46.51**	**16**	**2.91**		
Lack of Fit	**37.08**	**10**	**3.71**	**2.36**	**0.1527**
Pure Error	9.43	6	1.57		
Correlation	1059.68	30			

Developed model is considered to be adequate if R^2 value is high and standard error (SE) is low. The "lack of fit F-value" of 2.36 implies insignificant lack of fit. It can be clearly observed from the table that calculated F-value > tabulated F value at 95% confidence level. Thus the developed model is considered to be adequate. The predicted R-Square of 78.63% was in good conformity with the adjusted R-Square of 91.77%. Adequate precision value found to be 22.48 (ratio > 4).

Table 6: Results from ANOVA test for UTS

Response parameter Ultimate tensile strength (UTS)		
	Regression	**Residual**
S.S	1013.17	46.51
d.f	14	16
M.S	72.37	2.91
F-value Calculated	24.89	---
F-value Table	2.36	---
P-value	0.0	---
R^2	95.61%	---
Adjusted R^2	91.77%	---
Predicted R^2	78.63%	
Standard Error	0.64	---
Adequate Precision	22.48	---
Whether the model is adequate ?		**Yes**

SS: Sum of squares, d.f: Degree of freedom M.S: Mean squares, R^2: R square.

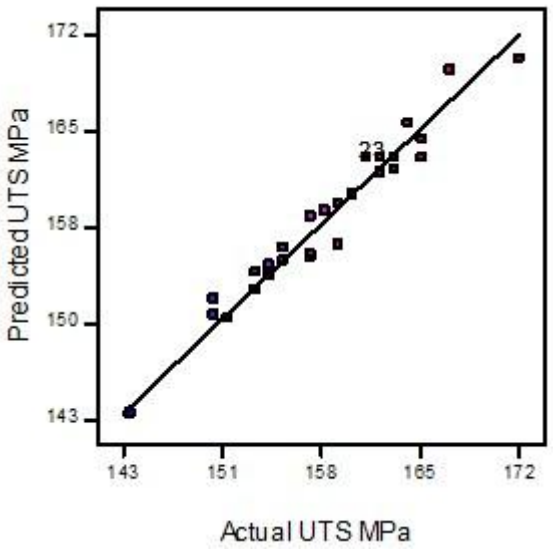

Figure 5: Scatter diagram actual Vs predicted values of UTS

From the Table 6, it is very clear to facilitate developed model is adequate and can be used for prediction of UTS response, with reasonable accuracy. A good agreement between calculated and observed values was found which further supports the adequacy of model. Scatter diagram as shown in Fig. 5 also validate the model, as the actual and predicted values are scattered on 45° line, signifying the perfect fitness of the model.

RESULTS AND DISCUSSIONS

The influence of process variables on UTS of weldments has been discussed and their effects on response have been presented in graphical form for better understanding.

Effect of tool rpm on UTS

The influence of tool rpm on ultimate tensile strength for different tool pin geometry is shown in Fig.6. Figure describes that UTS linearly increases with increase in tool rpm using threaded cylindrical tool. The minimum and maximum tensile strength achieved with threaded cylindrical tool was 138 MPa and 164 MPa respectively. Similar trends have been observed using triangular and taper cylindrical tools. At the minimum value of tool rotational speed i.e 1200 rpm, lower value of tensile strength was achieved due to poor frictional heat generation which ultimately leads to poor plastic flow of the material in stir zone. At maximum rotational speed of 1600 rpm, threaded cylindrical tool pin resulted in tensile strength of 164 MPa due accelerated flow of plasticized material.

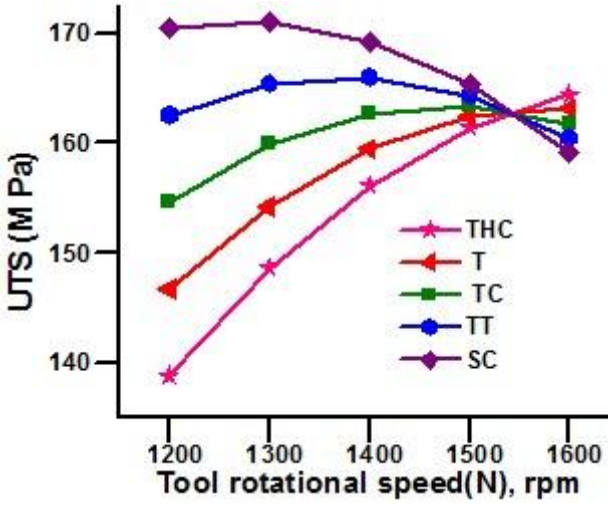

Figure 6: Effects of tool rpm on UTS

(at F=4kN, S= 30 mm/min)

At 1300 rpm straight cylindrical tool pin yielded maximum tensile strength of 172MPa due to better plastic flow of the material in stir zone. Threaded cylindrical tool pin profile produced lowest value of UTS 138 MPa at a tool rpm of 1200 rpm. This is due to less heat produced at low rpm resulted in poor plastic flow of material.

Effect of weld speed on UTS

The influence of weld speed on UTS is shown in Fig 7. It was revealed that UTS was least at lowest welding speed. As the speed of welding increased, UTS increased, attained a maximum value and after that decreased with further increase in speed of welding. Similar trends were observed with all types of tool geometry. At low welding speed heat input per unit length of weldment is high as reported as by Emam and Domiaty [27]. Due to high heat input, temperature in stir zone increases as a result slow cooling rate of stir zone leading to coarse grains responsible for low UTS. Further, at low weld speed grains having several sub boundaries which leads to decline in bond strength. This is the cause for low UTS of the joints at lower value of 10 mm/min weld speed. With an increment in weld speed, rubbing action between work piece and tool is enhanced. Heat generation in the weld zone is increased as interaction between work-piece and tool increased [28].

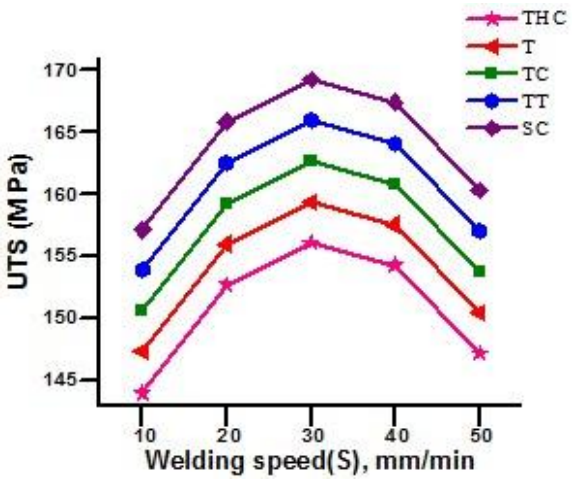

Figure 7: Effect of weld speed (mm/min) on UTS

(at F=4kN, N=1400 rpm)

Therefore 20-30 mm/min weld speeds gave higher values of UTS. The results are in consistency with the finding of Fushang Pan et al. [29].With further enhancement in welding speed, stir zone receives less amount of heat per unit length of weldment which is not sufficient for better material flow in plastic stage which creates lack of bonding and decline in tensile strength values at 40 mm/min and 50 mm/min.

Effect of axial force on UTS

Fig. 8 indicates the influence of axial force on UTS of welded joints fabricated using various pin geometries. It was observed that minimum UTS achieved with threaded cylindrical tool was 138 MPa at 2kN axial force. Heat produced is less and loss of heat from top surface of work material is more at low axial force and hence insufficient heat is available for plastic flow of material in stir zone resulting less bonding. Material from the weld cavity is lost as a flash as the shoulder is not able to confine the material

transferred in the weld cavity at lower axial force [30**].** It causes lower value of tensile strength. The transferred material is plasticized from advancing side to retreating side of the tool is restricted in the weld zone with further boost in downward axial force.

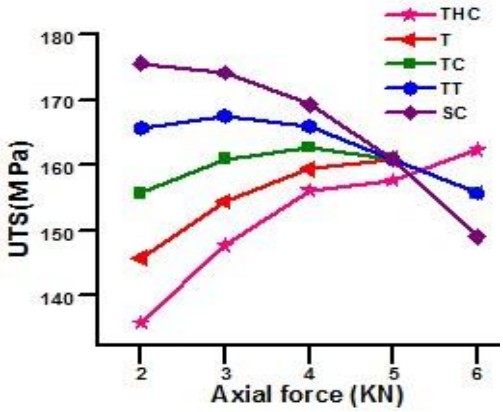

Figure 8: Effect of axial force on UTS

(at N= 1400 rpm, S=30 mm/min)

Furthermore, heat generated is higher with increment in axial force and heat loss is reduced. Because of the better work material entrapment within the weld zone for strong joint configuration which results in higher value of UTS for the weldments as in case of 3kN, 6kN axial forces with threaded cylindrical tool. At higher axial force 6kN because of extreme friction of tool shoulder and parent material, flash material carried away some heat from the work piece material. There is marginal decrement in heat availability for weld formation and hence at higher axial force 6kN UTS of the weld decreased. Similar trends have been observed using triangular and taper cylindrical pins. With straight cylindrical pin highest value of tensile strength, 176 MPa was observed at lowest axial force of 2kN and then regular decrease in UTS was observed. This is due to fact that the straight cylindrical tool without screw threads produces lesser amount of heat and under low axial force, forging action is insufficient for proper bonding leading to low UTS [31].

Effect of pin geometry on UTS

Fig. 6, 7 and 8 indicates the result of tool pin profiles on tensile strength at various process parameters. From these figures it is very clear that straight cylindrical pin produced maximum tensile strength at any values of tool rpm, welding speed and axial force while threaded cylindrical pin produced the joints having minimum tensile strength. It may be attributed to the fact that threaded cylindrical pin produces more frictional heat, temperature at the stir zone is high causing slow cooling rate results in coarse grains responsible for low tensile strength. Due to low heat input produced by straight cylindrical pin and owing to fast cooling rate grains produced were fine leading to improved tensile strength. Similar observations had been reported by [31].Hence the performance of straight cylindrical pin among all other pins used is considered to be the best.

Interactive effect of weld speed and tool rpm on UTS

Fig.9 describes the combined interactive effect of weld speed and tool rpm on UTS. Figure reveals that tensile strength increases from 147.3 MPa to 162.24 MPa with increase in tool rpm from 1200 rpm to 1600 rpm at weld speed of 20 mm/min. As the tool rpm increases from 1200 rpm to 1600 rpm at weld speed of 30 mm/min, no change in UTS was observed. Further, it is concluded that the UTS increased from 147.6 MPa to 156.6 MPa with increase in weld speed from 20 to 40 mm/min, while other parameters were constant.

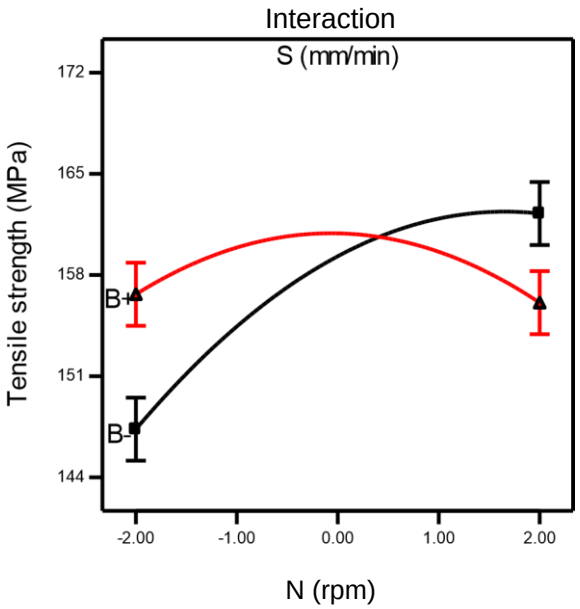

Figure 9: Interactive effect of weld speed and tool rpm on UTS

The improvement in UTS by increment in weld speed is due to the reason that increment in weld speed, decreased heat

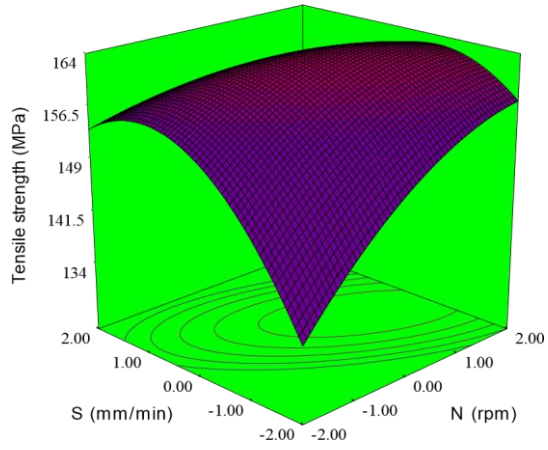

Figure 10: Response surface for UTS due to interaction of weld speed and tool rpm

input and process temperature, hence less time is available for grain growth. Fine grains results in increased tensile strength. Fig.14 (a) coarse grains and Fig.13 (b) shows the fine grained microstructure obtained at low and high weld speeds. The Response surface for tensile strength due to interaction of weld speed and tool rpm on UTS is shown in Fig. 10.

Interactive effect of weld speed and axial force on UTS

Fig.11 describes interactive effect of weld speed and axial force on UTS. It was observed that tensile strength increases from 145.6 MPa to 155.5 MPa with increase in weld speed from 10 to 50 mm/min at axial force of 3kN. The figure also represents that when axial force was incremented from 3kN to 5kN, UTS increased from 145.6 MPa to 152.1 MPa. It was recognized that heat generation is more with higher axial force as a result, plasticized material is transferred from advancing side to retreating side of the tool which is confined in the weld nugget.

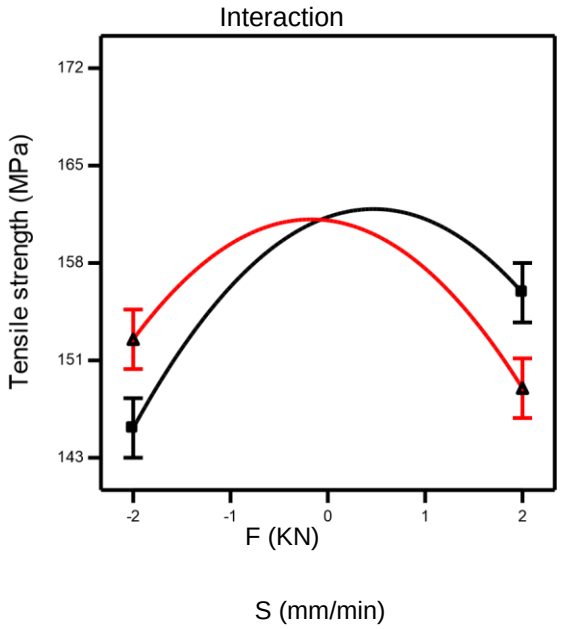

Figure 11: Interactive effect of weld speed and axial force on UTS

Therefore sufficient amount of heat is available for weld formation in stir zone resulting increase in tensile strength. Further it revealed that UTS value reaches to a highest value and then decreases to 148.5 MPa with increasing welding speed at 5kN axial force. This is due to the fact that at higher axial force more heat is generated as well as loss of heat reduced due to entrapment of the work material in the stir zone due to which heat input and temperature is very high and cooling rate is low so there is a time for grain coarsening which results lower UTS. The response surface plot for UTS due to the interaction of weld speed and axial force on UTS is indicated in Fig. 12.

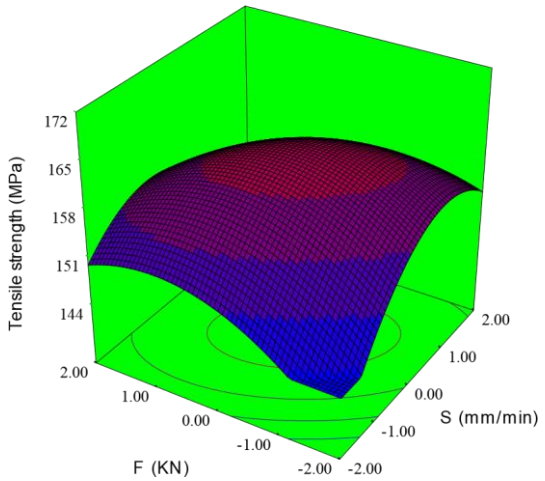

Figure 12: Response surface for UTS due to interaction of welding speed and axial force

SEM analysis of joints

The scanning electron microscope analysis was carried out to reveal the changes in microstructure of the joints after FSW.

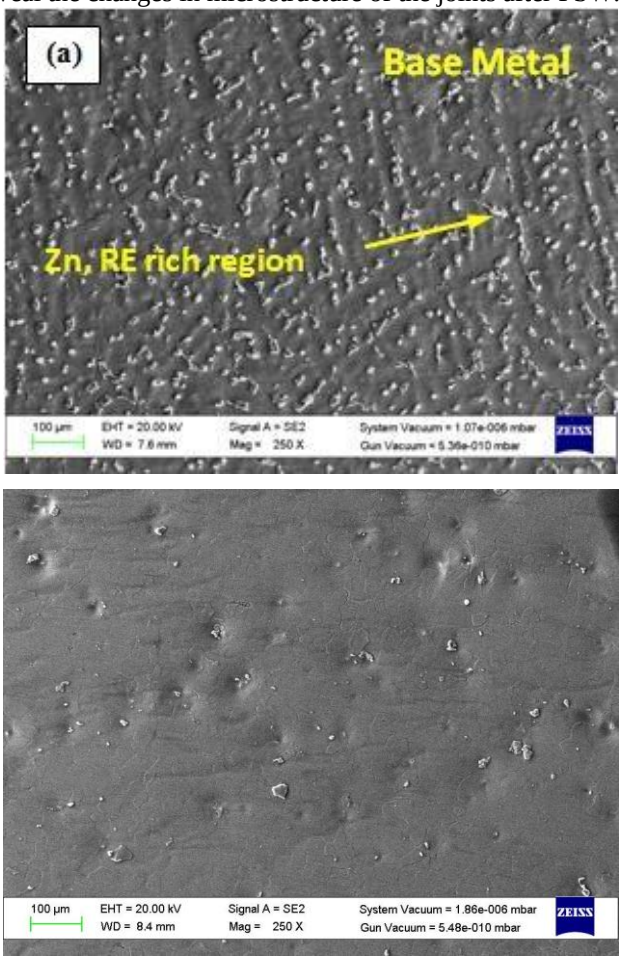

(b)

Figure 13: SEM micrographs at 250 X **(a)** Base metal **(b)** stir zone of the joint welded by straight cylindrical pin

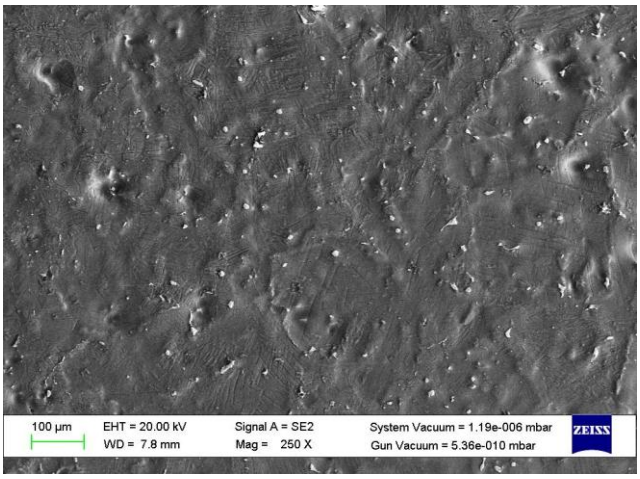

(a)

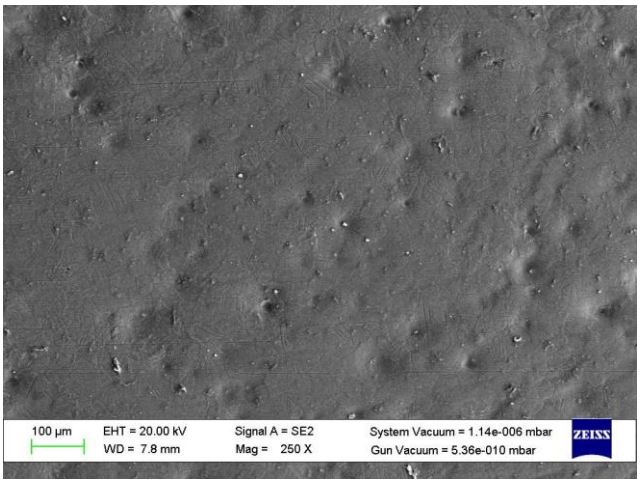

(b)

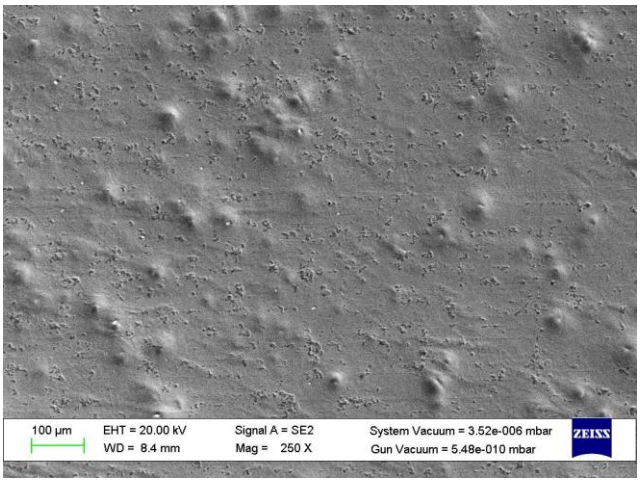

(c)

Figure 14: SEM micrographs at 250X **(a)** stir zone of joint welded by threaded cylindrical pin **(b)** triangular pin **(c)** taper cylinderical pin profile

The base material SEM micrograph is shown in Fig. 13. BM micrographs showed coarse grains with network of rare earth rich precipitates along with grainboundaries.After friction stir welding the cloudy Zn RE region converted into fine grains due to FSW, and grain refining abilty of Zr, as reported by [5] Zr can reduce the 80% grain size even at normal cooling rates for Mg alloys. Fig.13 (b) shows that, in stir zone the coarse and elongated rich cloudes of Zn and rare earth were fragmented mechanically into very fine sized grains which further produced good metallurgical bond, which causes superior tensile strength. Fig.14 indicates the presence of fine grains in the stir zone for the joints welded by threaded cylindrical, triangular,taper cylindrical tool pin profiles.

CONCLUSIONS

1. Five tools having different pin geometry were selected which are capable for joining Mg ZE41 alloy successfully using FSW process.
2. The FSW tool having straight cylindrical pin geometry produced the joints having maximum tensile strength.
3. Using experimental data generated, the regression modeling equation is developed which can effectively be used for predicting UTS of FS welded joints at 95% level of confidence.
4. Straight cylindrical pin profile produced highest tensile strength of 172 MPa at 1300 rpm, weld speed 30 mm/min and axial force 4kN.
5. The tool rpm has an intense effect on UTS of the weldments. The enhancement in tool rpm leads to increase in ultimate tensile strength using threaded cylindrical pin geometry.
6. The UTS increased with increment in weld speed, then reached highest value followed by decrease with all pin profiles.
7. The performance of straight cylindrical pin is considered to be the best in comparison to its counterparts for achieving maximum tensile strength.

ACKNOWLEDGEMENTS

Authors are gratifying all the faculty and staff members, Director CEMAJOR Annamalai University for extending their machines and equipment to carry out the research. The help provided by faculty and staff of material science lab of IIT Ropar is gratefully acknowledged.

REFERENCES

[1] Cao, X. and Jahazi, M., 2009. Effect of welding speed on the quality of friction stir welded butt joints of a magnesium alloy. Materials & Design, 30(6), pp.2033-2042.

[2] Padmanaban, G. and Balasubramanian, V., 2009. Selection of FSW tool pin profile, shoulder diameter and material for joining AZ31B magnesium alloy–an experimental approach. Materials & Design, 30(7), pp.2647-2656.

[3] Rodriguez, R.I., Jordon, J.B., Rao, H.M., Badarinarayan, H., Yuan, W., El Kadiri, H. and Allison, P.G., 2014. Microstructure, texture, and mechanical properties of friction stir spot welded rare-earth containing ZEK100 magnesium alloy sheets. Materials Science and Engineering: A, 618, pp.637-644.

[4] Luo, Z.A., Xie, G.M., Ma, Z.Y., Wang, G.L. and Wang, G.D., 2013. Effect of yttrium addition on microstructural characteristics and super plastic behavior of friction stir processed ZK60 alloy. Journal of Materials Science & Technology, 29(12), pp.1116-1122.

[5] Wang, C., Sun, M., Zheng, F., Peng, L. and Ding, W., 2014. Improvement in grain refinement efficiency of Mg–Zr master alloy for magnesium alloy by friction stir processing. Journal of Magnesium and Alloys, 2(3), pp.239-244. [6] Liu, Liming. 2010, "Welding and joining of magnesium alloys." Woodhead publishing limited, India, pp. 3-7.

[7] Zhang, H., Lin, S.B., Wu, L., Feng, J.C. and Ma, S.L., 2006. Defects formation procedure and mathematic model for defect free friction stir welding of magnesium alloy. Materials & design, 27(9), pp.805-809.

[8] Carlone, P. and Palazzo, G.S., 2015. Characterization of TIG and FSW weldings in cast ZE41A magnesium alloy. Journal of Materials Processing Technology, 215, pp.87-94.

[9] Dobriyal, R.P., Dhindaw, B.K., Muthu kumaran, S. and Mukherjee, S.K., 2008. Microstructure and properties of friction stir butt-welded AE42 magnesium alloy. Materials Science and Engineering: A, 477(1-2), pp.243-249.

[10] Chai, F., Zhang, D. and Li, Y., 2015. Microstructures and tensile properties of submerged friction stir processed AZ91 magnesium alloy. Journal of Magnesium and Alloys, 3(3), pp.203-209.

[11] Ugender, S., Kumar, A. and Reddy, A.S., 2014. Microstructure and mechanical properties of AZ31B magnesium alloy by friction stir welding. Procedia Materials Science, 6, pp.1600-1609.

[12] Singh, I., Cheema, G.S. and Kang, A.S., 2014.An experimental approach to study the effect of welding parameters on similar friction stir welded joints of AZ31B-O Mg alloy. Procedia engineering, 97, pp.837-846.

[13] Sun, S.J., Kim, J.S., Lee, W.G., Lim, J.Y., Go, Y. and Kim, Y.M., 2017. Influence of Friction Stir Welding on Mechanical Properties of Butt Joints of AZ61 Magnesium Alloy. Advances in Materials Science and Engineering, 2017.

[14] Commin, L., Dumont, M., Masse, J.E. and Barrallier, L., 2009. Friction stir welding of AZ31 magnesium alloy rolled sheets: Influence of processing parameters. Acta Materialia , 57(2), pp.326-334.

[15] Sahu, P.K. and Pal, S., 2015. Multi-response optimization of process parameters in friction stir welded AM20 magnesium alloy by Taguchi grey relational analysis. Journal of Magnesium and Alloys, 3(1), pp.36-46.

[16] Montgomery D C. Design and analysis of Experiments [M] 8th edition. New York: John Wiley and Sons, 2013.

[17] Sankar, B.R. and Umamaheswarrao, P., 2017. Modelling and Optimisation of Friction Stir Welding on AA6061 Alloy. Materials Today: Proceedings, 4(8), pp.7448-7456.

[18] Singh, G., Singh, K. and Singh, J., 2014. Modelling of the Effect of Process Parameters on Tensile Strength of Friction Stir Welded Aluminium Alloy Joints. Experimental Techniques, 38(3), pp.63-71.

[19] Rose, A.R., Manisekar, K. and Balasubramanian, V., 2011. Effect of axial force on microstructure and tensile properties of friction stir welded AZ61A magnesium alloy. Transactions of Nonferrous Metals Society of China, 21(5), pp.974-984.

[20] Gulati, P., Shukla, D.K. and Gupta, A., 2017. Defect formation analysis of Friction Stir welded Magnesium AZ31B alloy. Materials Today: Proceedings, 4(2), pp.1005-1012.

[21] Li, W.Y., Fu, T., Hütsch, L., Hilgert, J., Wang, F.F., Dos Santos, J.F. and Huber, N., 2014. Effects of tool rotational and welding speed on microstructure and mechanical properties of bobbin-tool friction-stir welded Mg AZ31. Materials & Design, 64, pp.714720.

[22] Sunil, B.R., Reddy, G.P.K., Mounika, A.S.N., Sree, P.N., Pinneswari, P.R., Ambica, I., Babu, R.A. and Amarnadh, P., 2015. Joining of AZ31 and AZ91 Mg alloys by friction stir welding. Journal of Magnesium and Alloys, 3(4), pp.330-334.

[23] Han, J., Chen, J., Peng, L., Tan, S., Wu, Y., Zheng, F. and Yi, H., 2017. Microstructure, texture and

mechanical properties of friction stir processed Mg14Gd alloys. Materials & Design, 130, pp.90-102.

[24] Patel, N., Bhatt, K.D. and Mehta, V., 2016. Influence of Tool Pin Profile and Welding Parameter on Tensile Strength of Magnesium Alloy AZ91 During FSW. Procedia Technology, 23, pp.558-565.

[25] Hung, F.Y., Shih, C.C., Chen, L.H. and Lui, T.S., 2007. Microstructures and high temperature mechanical properties of friction stirred AZ31–Mg alloy. Journal of Alloys and Compounds, 428(1-2), pp.106-114.

[26] Afrin, N., Chen, D.L., Cao, X. and Jahazi, M., 2008. Microstructure and tensile properties of friction stir welded AZ31B magnesium alloy. Materials Science and Engineering: A, 472(1-2), pp.179-186.

[27] Emam, S.A. and Domiaty, A.E., 2009. A refined energy-based model for friction-stir welding. World Academy of Science, Engineering and Technology, 29, pp.1010-1016.

[28] Ghosh, M., Kumar, K., Kailas, S.V. and Ray, A.K., 2010.Optimization of friction stir welding parameters for dissimilar aluminum alloys. Materials & Design, 31(6), pp.3033-3037.

[29] Pan, F., Xu, A., Deng, D., Ye, J., Jiang, X., Tang, A. and Ran, Y., 2016. Effects of friction stir welding on microstructure and mechanical properties of magnesium alloy Mg-5Al-3Sn. Materials & Design, 110, pp.266-274.

[30] Raja kumar, S., Muralidharan, C. and Balasubramanian, V., 2011. Influence of friction stir welding process and tool parameters on strength properties of AA7075-T6 aluminium alloy joints. Materials & Design, 32(2), pp.535-549.

[31] Motalleb-Nejad, P., Saeid, T., Heidarzadeh, A., Darzi, K. and Ashjari, M., 2014. Effect of tool pin profile on microstructure and mechanical properties of friction stir welded AZ31B magnesium alloy. Materials & Design, 59, pp.221-226.